Jurnal Teknologi

Full Paper

PREDICTION OF SOIL SETTLEMENT ON SOFT CLAY SOIL USING NORMALIZED ROTATIONAL MULTIPLE YIELD SURFACE FRAMEWORK (NRMYSF)

Hamzah Abd. Hamid[a]*, Mohd Jamaludin Md. Noor[a], Rohaya Alias[b], Asmidar Alias[b]

[a]School of Civil Engineering, College of Engineering, UiTM Shah Alam, 40450, Selangor, Malaysia
[b]School of Civil Engineering, College of Engineering, UiTM Jengka, 26400, Pahang, Malaysia

Article history
Received
11 April 2022
Received in revised form
11 September 2022
Accepted
18 September 2022
Published Online
26 December 2022

*Corresponding author
rohaya_alias@uitm.edu.my

Graphical abstract

Abstract

Soft clays are highly compressible, high-water content, low shear strength, and have poor permeability, which result in significant settlement under long-term loads. Therefore, one of the most challenging geotechnical engineering problems is to predict the settlement from soft clay soil. Normalized Rotational Multiple Yield Surface Framework (NRMYSF) is developed from the soil stress-strain behaviour and shear strength characteristic. It is able to estimate the stress-strain curve for shear strength in triaxial tests. The consolidated drained (CD) triaxial tests and conventional 1-dimensional consolidation of oedometer has been conducted on soft clay soil. The settlement soil prediction was compared between the NRMYSF and conventional 1-dimensional consolidation under Terzaghi's principle. The NRMYSF prediction model was smaller than the conventional oedometer by 0.1459m to 0.1431m for Sample A, and by 0.1890m to 0.1398m for Sample B. Therefore, this method has the potential to predict the settlement of soft clay soils.

Keywords: Settlement Soil, Soft Clay, NRMYSF, Triaxial, Oedometer

Abstrak

Tanah liat lembut mempunyai kemampatan, kandungan air yang tinggi, kekuatan ricih yang rendah, dan mempunyai kebolehtelapan yang rendah, yang mengakibatkan mendapan yang ketara di bawah beban jangka panjang. Oleh itu, salah satu masalah kejuruteraan geoteknikal yang paling mencabar adalah untuk meramalkan pemendapan dari tanah liat lembut. Rangka Kerja Permukaan Berbilang Hasil Putaran Dinormalisasi (NRMYSF) dibangunkan daripada kelakuan tegangan-terikan dan ciri kekuatan ricih. Ia dapat meramalkan lengkung tegangan-terikan untuk kekuatan ricih dalam ujian triaksial. Ujian tiga paksi terkukuh salir (CD) dan 1 dimensi konvensional bagi oedometer telah dijalankan pada tanah liat lembut. Ramalan pemendapan tanah telah dibandingkan diantara NRMYSF dengan 1 dimensi konvensional di bawah prinsip Terzaghi. Model ramalan NRMYSF adalah lebih kecil daripada oedometer konvensional sebanyak 0.1459m hingga 0.1431m untuk Sampel A, dan sebanyak 0.1890m hingga 0.1398m untuk Sampel B. Oleh itu, kaedah ini berpotensi untuk meramalkan pemendapan tanah liat lembut.

Kata kunci: Kunci: Mendapan Tanah, Tanah Liat, NRMYSF, Triaksial, Oedometer

1.0 INTRODUCTION

Soft clay soil can be found along the East and West Coasts of Peninsular Malaysia [1]. These soils are problematic due to their low strength and high compressibility [21]. In soft clay areas, the settlement of soil poses a significant challenge because they are more prone to foundation damage. Typically, additives are used to minimize the effect of moisture content on the soil, such as shrinkage and swelling. For example, lime is used as an additive to improve bearing capacity and reduce volumetric instability which are found in pavements [23].

Soil settlement prediction is straightforward in theory, but in practice, it is challenging due to factors such as soil layer compressibility parameters that differ significantly from the actual scenario [6]. Two factors contribute to the difficulty of predicting soil settlement such as too many methods are not appropriate to the design problem encountered and engineer fails to assess the soil stiffness necessary for the most accurate forecast of settlement [7]. Terzaghi's theory of soil consolidation is a well-established method for predicting soil settlement [20]. This theory is based on the effective stress principle, which was developed from several ideal assumptions in order to obtain a simplified theory.

Consolidation theory states that excess pore water pressure dissipates when pressure is applied, which reduces the soil volume, and soil behaviour is assumed to be linearly elastic and one-dimensional consolidation. The theory is widely used because it is straightforward and capable of capturing many parameters. Despite its widespread use, it is not always practical due to uncertainty and constant parameter [5], [10], [11], [24].

On shallow foundations, the existing methods for soil prediction settlement depend on perfectly plastic soil constitutive behaviour while predicting the immediate settlement uses linear elastic soil behaviour. As a result, these approaches do not accurately reflect the soil non-linear stress-strain behaviour and underestimated the settlement [8], [15], [16], [18]. The actual settlement may differ from the predicted settlement in traditional consolidation analyses due to limitations and unrealistic assumptions.

Soil settlement was influenced by the stiffness of soil [2], [4], [9], [22]. The triaxial test has been proposed as an alternative to conventional oedometers for assessing soil settlement since the results for soil stiffness in the triaxial test are less affected by bedding errors. There are researchers who studied the relationship between shear strength and settlement in fine-grained soil [13], [17]. Pre-consolidation pressure in soils is closely associated with undrained shear strength [12].

Predicting soil settlements has been improved with the introduction of new methods or models. Despite these improvements, settlement capability prediction remains a mystery. The engineering examples show that settlement prediction and accurate calculation of soft soil subgrades are the biggest challenges in the construction of roadbeds on soft clay. Hence, this study was conducted to predict the settlement of soil based on the Normalized Rotational Multiple Yield Surface Framework (NRMYSF).

2.0 METHODOLOGY

The Normalized Rotational Multiple Yield Surface Framework (NRMYSF) is derived from the stress-strain soil behaviour and represents the true in-situ stress state. Furthermore, the framework considers the soil actual elastic-plastic response to stress. When the soil undergoes anisotropic settlement, the framework utilizes the increase in mobilizing shear strength. This framework was developed from actual of the soil stress-strain curve. NRMYSF is a semi-empirical model used to represent soil volume change while taking into account the true nature of the soil thus when effective stress decreases. The working model of NRMYSF is based on the development of shear strength and effective stress within a single framework.

NRMYSF consist of two (2) variables which are driving and resisting variables. The driving effective stress acted as driving parameter and the resisting variable is the mobilized shear strength envelope during compression. The mobilized shear strength envelope is taken as the nonlinear envelope rather than conventional linear characteristic. As the strain increased, both the mobilized shear strength and frictional angle increased. Shear strength increased due to the increase value of mobilized angle of friction ϕ. Figure 1 demonstrates the mobilized shear strength envelope calculated from soil stress-strain curves at various axial strains.

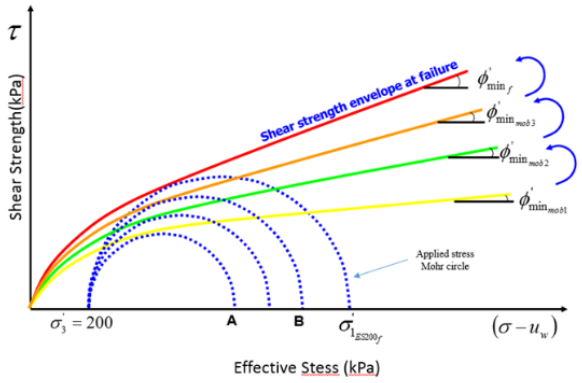

Figure 1 Enlargement of Mohr circle due to the increasing of effective stress [14], [19]

To predict volume change behaviour, RMYSF uses actual stress-strain and effective values. However, the axial strains at failure depend on the effective stress. The significant difference of axial strains at failure for each effective stress of specimens makes it

challenging to predict the stress-strain curves accurately. Hence, the RMYSF method has been refined and improved by introducing a new Normalized Rotational Multiple Yield Surface Framework (NRMYSF) method. In equation 1, the ratio of maximum strains value over the selected strains at failure were calculated. According to these researcher [3], [15], the new framework is capable to predict stress-strain curve better than RMYSF.

$$\text{Normalized strain ratio} = \frac{(\text{Max. } \varepsilon_f)}{(\text{Max. } \varepsilon_f \text{ (selected stress level)}} \quad [1]$$

The capability of NRMYSF to predict stress-strain curves at any effective stress will be used to predict the total settlement of soil in a thick soil formation by discretizing the soil into horizontal layers into smaller thicknesses. Nevertheless, the soil must be homogeneous at any depth to accurately predict. The mobilized shear strength envelope applies to the entire range of effective stresses. In other words, the soil intrinsic can be used to predict the stress-strain response at any effective stress or depth in the ground. The applied loading increased as well the effective stress of soil. The prediction of settlement by using NRMSF is calculated based on the difference of axial strain, as shown in equation 2.

$$\text{Settlement} = (\varepsilon_{af} - \varepsilon_{ai}) \times \text{layer thickness} \quad [2]$$

$\Delta\ \varepsilon_{af}$ = final strain of specimen
$\Delta\ \varepsilon_{ai}$ = initial strain of specimen

3.0 EXPERIMENTAL PROCEDURE

The undisturbed soil samples were collected by using a Shelby tube sampler. The samples were taken from Kampung Sungai Jaya, Bukit Gambir, Muar at a 1.0 m depth from the surface to represent in-situ soil. The tube was used with a diameter of 70 mm and a length of 1000 mm, as shown in Figure 2. The in-situ moisture content was recorded. All testing, such as physical and geotechnical engineering properties, follows British Standard.

All samples were carefully extruded from the tube to prevent disturbed conditions. Two (2) sets of tests for triaxial and consolidation were prepared. The study was conducted by using the consolidated drained (CD) triaxial test in fully saturated conditions on 50 mm diameter and 100 mm height specimens. All specimens were applied to saturation stage, consolidation and shearing at the rate of less than or equal to 0.01 mm/min. The shearing rate was calculated after pore water pressure dissipated by at least 95% during the consolidation stage. The effective pressure of 50 kPa, 100 kPa, and 200 kPa was applied to obtain the Mohr circle. The conventional 1-dimensional (1D) consolidation was conducted on the saturated cylindrical specimen using an oedometer test in fully saturated condition with 50 mm diameter and 20 mm height. The sequence loading uses 6.25 kPa, 12.5 kPa, 25 kPa, 50 kPa, 100 kPa, 200 kPa, 400 kPa, 800 kPa and 1600 kPa increments.

Figure 2 Thin-wall Tube

4.0 RESULT AND DISCUSSION

The soil colour was dark grey, and the in-situ moisture content with average of 47.75 % and the specific gravity for the soil was 2.51. In the particle size distribution analyses, the dry sieving and wet sieving were conducted since more than 10% of fines exist within the soil. Therefore, the soil can be categorized as FINE soil based on the sieve analysis, where clay particles dominate at 58.25%. A further test was conducted, such as the Atterberg limit tests, to determine the consistency and plasticity. The studied soils were summarized in Table 1. As a result, the studied soil was classified as FINE soil with high plasticity clay (CH) according to Whitlow (2004) and Table 2 summarized geotechnical properties for the studied soil.

Table 1 Physical properties for undisturbed soft clay from Muar

Test	Value	Group
Natural Moisture Content (%)	47.75	
Particle Size Distribution (PSD)		
Gravel (%)	0	
Sand (%)	10.50	
Silt (%)	31.25	FINE soil with *High Plasticity Clay* (CH)
Clay (%)	58.25	
Atterberg Limit		
Liquid Limit (%)	63	
Plastic Limit (%)	30	
Plastic Index (%)	33	
Specific Gravity (G_s)	2.51	

Table 2 Geotechnical properties for undisturbed soft clay from Muar

Test	Sample A	Sample B
1-D Consolidation Oedometer		
Pre-consolidation (kPa)	50	44
Compression Index (C_c)	0.436	0.530
Recompression Index (C_R)	0.084	0.120
Oedometric Modulus (E_{od})	957	744
Bulk Density (Mg/m^3)	1.752	1.757
Void Ratio (*e*)	1.106	1.102
Moisture Content (%)	47.0	47.1
Poisson ratio, *v*	0.500	0.500
Consolidation Drained (CD) Triaxial		
Cohesion, C_u (kPa)	28	30
Frictional Angle (ϕ)	23	23

The triaxial test were conducted at different effective stresses of 50 kPa, 100 kPa and 200 kPa. For Sample A and Sample B, the stress-strain relationship and maximum deviator stress at failure were shown in Figure 3(a) and Figure 4(a). Table 3 summarized these samples failure condition shearing stage in the triaxial test. These values are then used to draw the Mohr circle envelope as shown in Figure 3(b) and Figure 4(b). As can be seen in this observation, the curvilinear shear strength envelope covers all ranges of effective stress compared to the linear envelope, and it prevents any errors in shear strength estimation over the entire stress range. The smallest Mohr's circle at low effective has been ignored using the linear shear strength envelope, which affects the strength and underestimates the soil settlement. The estimation of shear strength under the same effective stress was analyzed. It is shown that using a curvilinear envelope gives the soil greater strength than a linear envelope of shear strength. Table 4 shows the shear strength estimation difference based on a different envelope.

Table 3 Failure Condition in Shearing Stage for Consolidated Undrained (CD-A&B) Triaxial Test

Failure Condition	50 kPa	100 kPa	200 kPa
Triaxial CD- Sample A			
Axial Strain (%)	14.64	17.51	14.47
Minor Principal Stresses, σ_1 (kPa)	50	100	200
Major Principal Stresses, σ_3 (kPa)	172.8	313.1	544.2
Deviator Stress (σ_3- σ_1) (kPa)	122.8	213.0	344.2
Triaxial CD- Sample B			
Axial Strain (%)	20.03	16.77	14.25
Minor Principal Stresses, σ_1 (kPa)	50	100	200
Major Principal Stresses, σ_3 (kPa)	189.9	319.1	547.9
Deviator Stress (σ_3- σ_1) (kPa)	139.9	219.1	347.9

Table 4 Shear Strength Estimation Under Different Envelope

Sample	Linear Interpretation				Curvilinear Interpretation		
	c	°	(σ-u_w)	τ	°	(σ-u_w)	τ
Sample CD-A	28.3	23.1	255	131	21.0	255	140
Sample CD-B	30.1	22.8	258	132	18.5	255	144

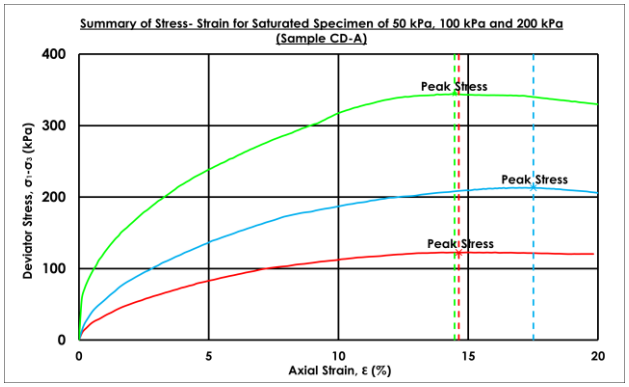

(a)

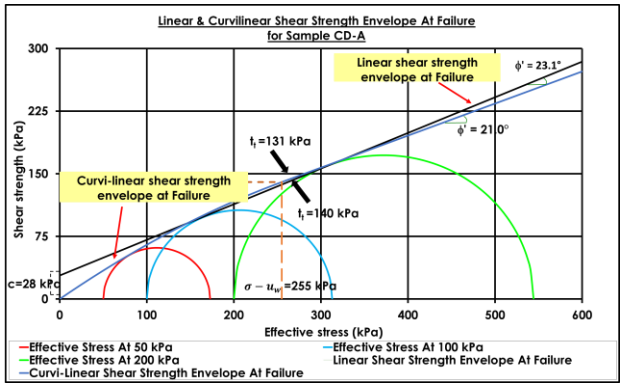

(b)

Figure 3 (a) Stress strain curve for saturated sample A (b) Non-linear Mohr circle envelope for saturated sample CD-A

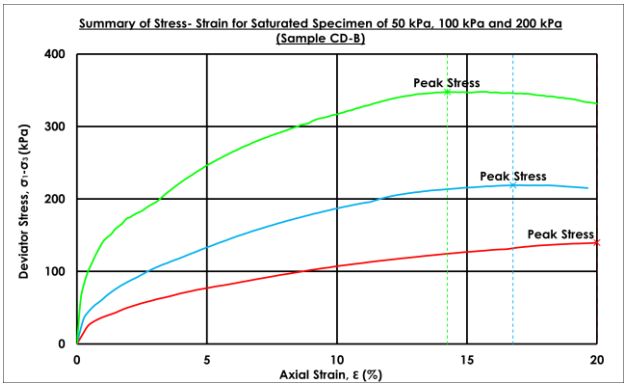

(a)

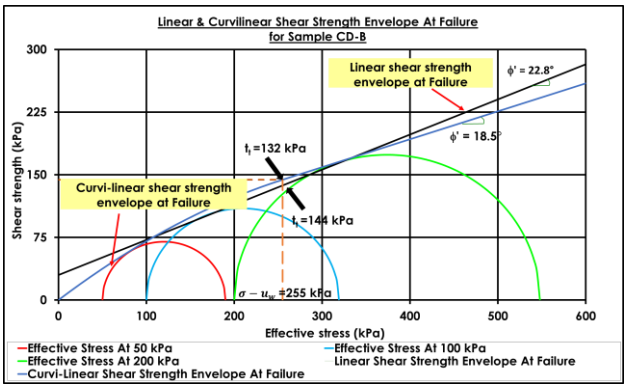

(b)

Figure 4 (a) Stress strain curve for saturated sample B (b) Non-linear Mohr circle envelope for saturated sample CD-B

Despite its ability to predict stress-strain behaviour at any effective stress, the Rotational Multiple Result Surface Framework has limitations. At different values of axial strains, the maximum deviator stresses at failure depend on the effective stresses during shearing, leading to large percentage errors during prediction. The RMYSF method has been refined with a new technique known as the Normalized Rotational Multiple Yield Surface Framework (NRMYSF) introduced by [15]. Table 5 shows that the value of strain at maximum deviator stress was

selected and used as the numerator to normalize the data for other effective stresses by using Equation 1. The curvilinear envelopes in Figure 5(a) and Figure 6(a) were predicted under RMYSF, while the curvilinear envelopes in Figure 5(b) and Figure 6(b) were predicted under NRMYS.

Table 5 Normalized axial strain for Sample A and Sample B with effective stress of 50 kPa, 100 kPa and 200 kPa

Effective Stress	RMYSF	Normalized Conversion Factor	NRMYSF
Triaxial CD- Sample A			
Effective Stress - 50 kPa	14.64	1.20	17.51
Effective Stress - 100 kPa	17.51	1.00	17.51
Effective Stress - 200 kPa	14.47	1.21	17.51
Triaxial CD- Sample B			
Effective Stress - 50 kPa	20.03	1.00	20.03
Effective Stress - 100 kPa	16.77	1.19	20.03
Effective Stress - 200 kPa	14.25	1.41	20.03

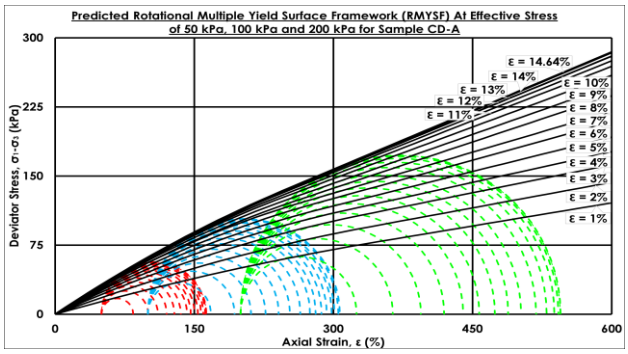

(a)

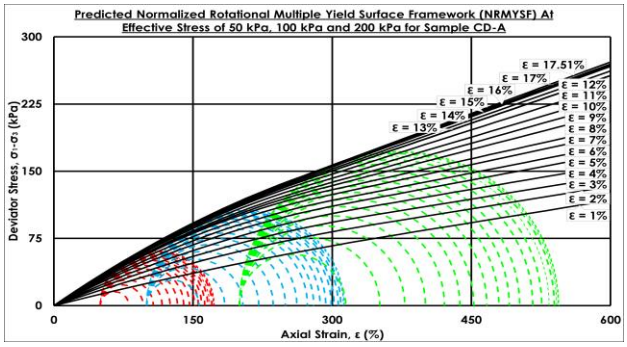

(b)

Figure 5 (a) Predicted RMYSF with various effective stress for Sample A (b) Predicted NRMYSF with various effective stress for Sample A

From the curvilinear envelope established from Figure 5 and Figure 6, the stress-strain curves were predicted under RMYSF and NRMYS as shown in Figure 7(a)(b) and Figure 8(a)(b). Tables 6 and 7 show the percentage error for the predicted and experimental data, respectively. The inverse normalized strain value gives an excellent match to the actual laboratory data. As a result, the average percentage error for Sample CD-A and Sample CD-B decreased from 3.51% to 1.64% and 2.77% to 1.41%, respectively. This similar to the result by [3], [15]. The new framework is capable to predict stress-strain curve better than RMYSF. Lower percentage values indicate that predictions matched the laboratory results.

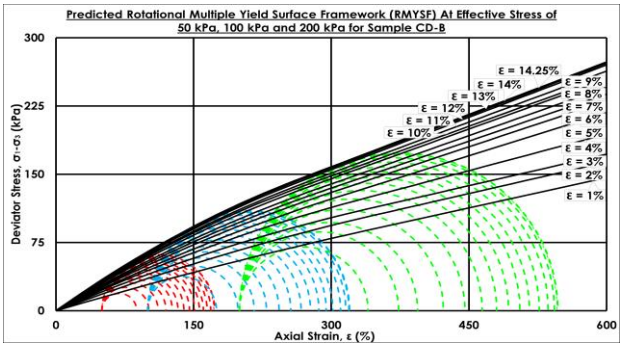

(a)

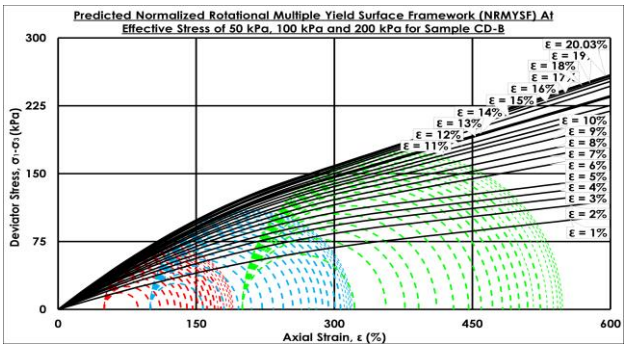

(b)

Figure 6 (a) Predicted RMYSF with various effective stress for Sample B (b) Predicted NRMYSF with various effective stress for Sample B

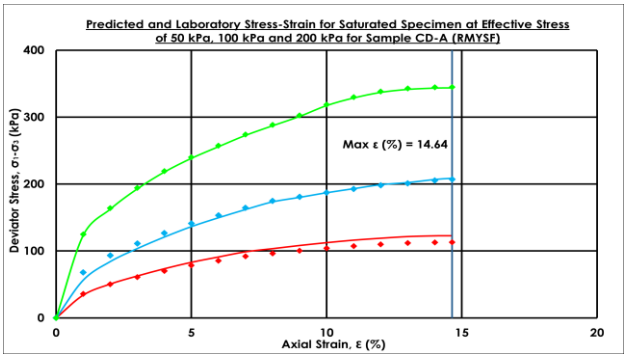

(a)

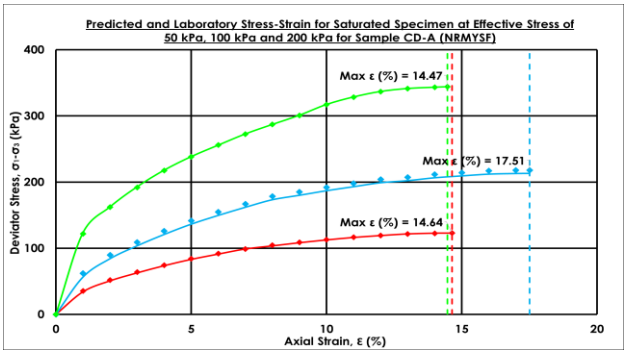

(b)

Figure 7 (a) Predicted and laboratory stress-strain behaviour for Sample A under RMYSF (b) Predicted and laboratory stress-strain behaviour for Sample A under NRMYSF

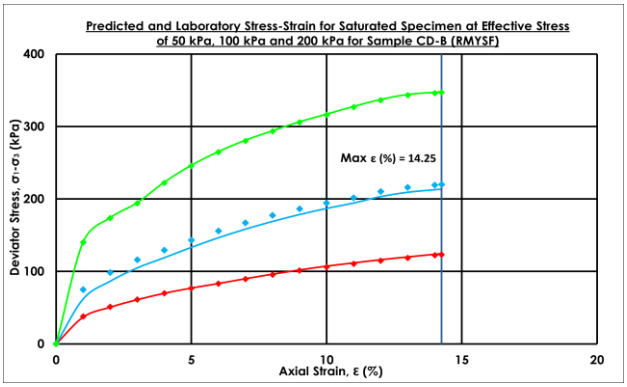

(a)

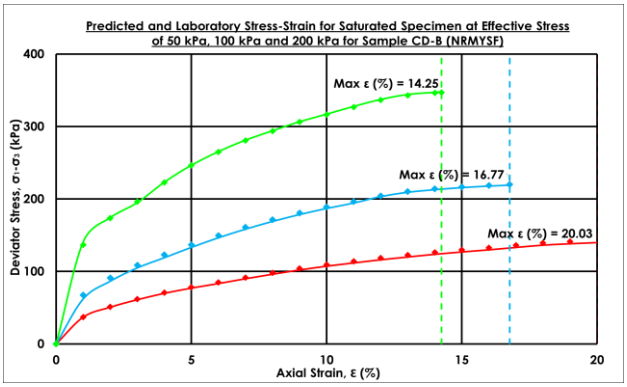

(b)

Figure 8 (a) Predicted and laboratory stress-strain behaviour for Sample B under RMYSF (b) Predicted and laboratory stress-strain behaviour for Sample B under NRMYSF

Table 6 Percentages Error Under RMYSF

RMSYF						
Sample	**Percentage Error CD-A**			**Percentage Error CD-B**		
Axial Strain (%)	**50 kPa**	**100 kPa**	**200 kPa**	**50 kPa**	**100 kPa**	**200 kPa**
1	5.44	20.55	1.26	2.54	20.60	0.56
2	0.62	10.93	0.92	1.09	13.60	0.46
3	3.02	7.26	0.75	0.42	10.47	0.42
4	4.51	4.99	0.65	0.01	8.73	0.37
5	5.50	3.44	0.58	0.25	7.34	0.34
6	6.17	2.37	0.53	0.45	6.29	0.32
7	6.72	1.54	0.48	0.63	5.50	0.31
8	7.01	0.87	0.45	0.77	4.89	0.29
9	7.28	0.51	0.42	0.89	4.40	0.29
10	7.50	0.17	0.39	0.98	4.02	0.28
11	7.68	0.10	0.37	1.06	3.70	0.27
12	7.81	0.36	0.36	1.13	3.35	0.26
13	7.92	0.49	0.35	1.18	3.13	0.26
14	7.97	0.67	0.35	1.23	3.01	0.26
Percentage Error (%)	**6.08**	**3.87**	**0.56**	**0.90**	**7.08**	**0.33**
Total Percentage Error (%)	**3.51**			**2.77**		

Table 7 Percentages Error Under NRMYSF

NRMSYF						
Sample	**Percentage Error CD-A**			**Percentage Error CD-B**		
Axial Strain (%)	**50 kPa**	**100 kPa**	**200 kPa**	**50 kPa**	**100 kPa**	**200 kPa**
1	3.95	9.91	1.37	0.16	8.22	2.86
2	2.47	6.51	0.23	0.72	5.14	0.40
3	1.91	5.21	0.53	1.12	3.32	0.71
4	1.22	4.41	0.31	1.37	3.30	0.19
5	1.07	3.86	0.17	1.53	2.52	0.04
6	0.86	3.49	0.05	1.65	1.96	0.19
7	0.10	3.19	0.12	1.75	1.63	0.15
8	0.94	2.96	0.05	1.84	1.32	0.14
9	0.58	2.83	0.16	1.91	1.11	0.02
10	0.42	2.71	0.11	1.97	0.98	0.19
11	0.26	2.61	0.16	2.01	0.93	0.31
12	0.05	2.52	0.14	2.05	0.43	0.23
13	0.10	2.48	0.11	2.09	0.41	0.38
14	0.11	2.42	0.05	2.12	0.47	0.21
15		2.38		2.14	0.43	
16		2.34		2.16	0.37	
17		2.33		2.19		
18				2.21		
19				2.22		
20				2.23		
Percentage Error (%)	**1.00**	**3.66**	**0.25**	**1.77**	**2.03**	**0.43**
Total Percentage Error (%)	**1.64**			**1.41**		

Due to the ability of NRMYSF to foresee stress-strain behaviour more accurately under any effective stress, this method was used in the prediction of settlement soil. As mentioned in Section 3, the soil settlement model was designed with a homogeneous layer of soil with a depth of 10m. The loading of 10 kN/m^2 with a thickness of 1m was applied to the soil formation. The soil layer is separated into five equal layers, with each layer being 2 meters thick. The groundwater table (GWT) was assumed to be 0 meters below the surface. Figure 9 shows the scenario of the setting for the settlement analysis.

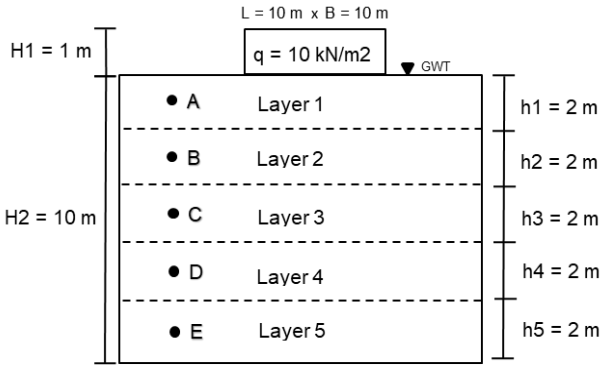

Figure 9 Soil settlement modelling simulation were developed

At the initial effective stress, the effective stress was calculated without any load application. The application of loading on the soil increased the effective stress and was calculated as final effective stress. At the mid-height of each layer, the initial and final effective stress was calculated, as shown in Table 8. The same effective stress was also applied on the prediction strain-stress curve under the NRMYSF method for shears strength.

Table 8 Calculated Initial Effective Stress, σ_{avi} and Final Effective Stress, σ_{avf}

Depth (m)	Initial Effective Stress, σ_{avi}	Final Effective Stress, σ_{avf}
1	10.60	20.54
3	31.80	40.72
5	53.00	60.01
7	74.20	79.42
9	95.40	99.28

Figure 10, Figure 11, Figure 12 and Figure 13 shows the soil settlement modelling based on the Normalized Rotational Multiple Yield Surface Framework (NRMYSF) at effective stress of 10.60 kPa, 31.80 kPa, 53.00 kPa, 74.20 kPa and 95.40 kPa. Later, the predicted strain-stress curve using this framework is shown in Figure 12 and Figure 13. The difference of axial strain between initial and final effective stress was measured to determine soil settlement. After that, it will be multiplied by the thickness of each layer which results in the soil settlement, as shown in Table 9 and Table 10. The observation shows that at lower net stress, the settlements are bigger than the settlement at high net stress. The prediction of soil settlement for samples CD-A and CD-B was 0.1431 m and 0.1398 m, respectively.

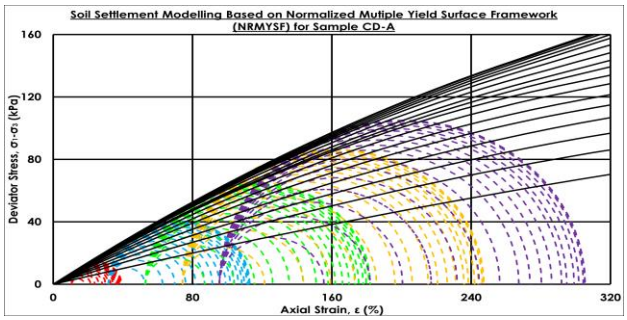

Figure 10 Soil settlement modelling at effective stress of 10.60 kPa, 31.80 kPa, 53.00 kPa, 74.20 kPa and 95.40 kPa for Sample CD-A

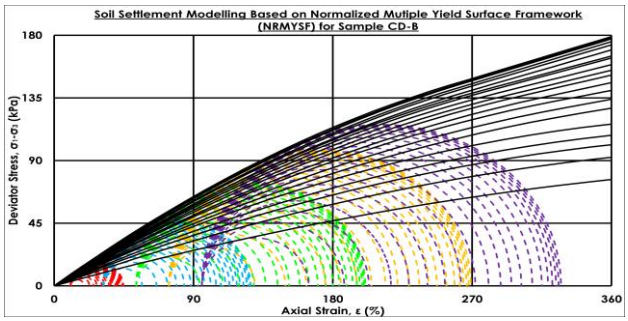

Figure 11 Soil settlement modelling at effective stress of 10.60 kPa, 31.80 kPa, 53.00 kPa, 74.20 kPa and 95.40 kPa for Sample CD-B

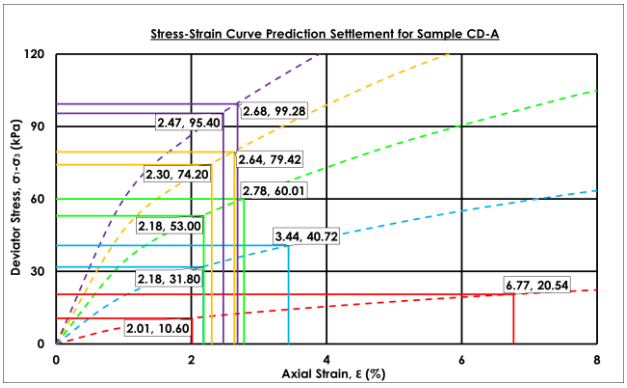

Figure 12 Predicted the strain-stress curve for Sample CD-A

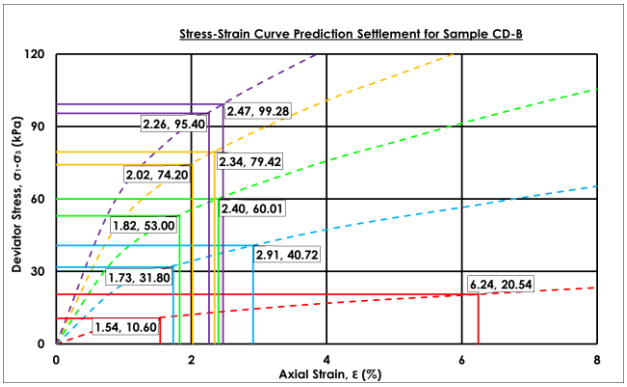

Figure 13 Predicted the strain-stress curve for Sample CD-B

Table 9 Prediction of Soil Settlement for Sample A

Sample CD-A			
Depth (m)	**Δε (%)**	**h, (m)**	**Settlement (m)**
1	4.76	2.00	0.0951
3	1.26	2.00	0.0252
5	0.59	2.00	0.0119
7	0.33	2.00	0.0067
9	0.21	2.00	0.0042
Total Settlement (m)			**0.1431**

Table 10 Prediction of Soil Settlement for Sample B

Sample CD-B			
Depth (m)	**Δε (%)**	**h, (m)**	**Settlement (m)**
1	4.70	2.00	0.0941
3	1.18	2.00	0.0236
5	0.57	2.00	0.0115
7	0.33	2.00	0.0065
9	0.21	2.00	0.0042
Total Settlement (m)			**0.1398**

7

The soil parameters used in the analysis of settlement soil were based on the soil tested under the oedometer test. The total settlement of the saturated soil consists of 3 components: immediate settlement, primary settlement, and secondary settlement. Therefore, the Poisson ratio, v and undrained modulus, Eu, is involved in calculating the immediate settlement soil. The calculations of immediate settlement soil are tabulated in Table 11.

Table 11 Prediction of Soil for Immediate Settlement (S_i)

Sample	Poisson ratio, v	Undrained Modulus, Eu (kN/m²)	Immediate Settlement, S_i (m)
Conso-A	0.5	957	0.072
Conso-B	0.5	744	0.093

The primary and secondary settlements were analyzed by using Terzaghi's theory. It was observed that during the primary settlement, the excess pore water pressure dissipates due to the applied load, while for the secondary settlement due to soil deformation after complete dissipation. It shows that the prediction of total settlement for Conso-A and Conso- B was 0.1459 m and 0.1890 m, respectively, as tabulated in Table 12 and Table 13. Table 14 shows the comparison of prediction settlement soil between conventional oedometer and triaxial shear strength. From the observation, it shows that the soil settlement prediction on NRMYS were smaller than traditional consolidation.

Table 12 Prediction of Total Settlement Under an Oedometer Test for Sample A

Sample Conso A					
Depth (m)	σ_{avi} (kN/m²)	σ_{avf} (kN/m²)	S_c (m)	S_s (m)	Settlement (m)
1	10.60	20.54	0.0229	0.0000	0.0229
3	31.80	40.72	0.0086	0.0001	0.0087
5	53.00	60.01	0.0223	0.0001	0.0224
7	74.20	79.42	0.0122	0.0002	0.0124
9	95.40	99.28	0.0720	0.0002	0.0074
		$\sum S_c + S_s$			0.0738
		$\sum S_i + S_c + S_s$			**0.1459**

Table 13 Prediction of Total Settlement Under an Oedometer Test for Sample B

Sample Conso B					
Depth (m)	σ_{avi} (kN/m²)	σ_{avf} (kN/m²)	S_c (m)	S_s (m)	Settlement (m)
1	10.60	20.54	0.0327	0.0001	0.0328
3	31.80	40.72	0.0122	0.0001	0.0123
5	53.00	60.01	0.0271	0.0002	0.0273
7	74.20	79.42	0.0148	0.0002	0.0150
9	95.40	99.28	0.0087	0.0002	0.0089
		$\sum S_c + S_s$			0.0963
		$\sum S_i + S_c + S_s$			**0.1890**

Table 14 Comparison Soil Settlement

Sample	Prediction Soil Settlement	
	Conventional Oedometer (m)	Triaxial (m)
A	0.1459	0.1431
B	0.1890	0.1398

5.0 CONCLUSION

Normalized Rotational Multiple Yield Surface Framework (NRMYSF) capable to improve the accuracy of predicting the stress-strain curve of soft clay soil obtained from Kampung Sungai Jaya, Bukit Gambir, Muar. The range of total percentage error was less 10%, thus providing good predictions compared with actual data recorded during the experiment. Normalized Rotational Multiple Yield Surface Framework (NRMYSF) can predict the settlement of undisturbed soil. It was discovered that the prediction utilizing this framework performed significantly better than Terzaghi's consolidation using the 1D-oedometer test.

Acknowledgement

The authors would like to gratitude the Ministry of Higher Education (MOHE) and the Institute of Research Management Institute (IRMI, UiTM) for providing financial assistance for this research. It is funded under the Fundamental Research Grant Scheme (FRGS).

References

[1] Ahmad, Juhaizad & Ikmal, Fazlan & Rahman, Abdul & Fithry Senin, Syahrul & Md Noor, Mohd Jamaludin. 2018. Volume Change Behaviour of Clay by Incorporating Shear Strength: A Review. *Proceedings of the Second International Conference on the Future of ASEAN (ICoFA) 2017*. 2: 495-503. DOI: https://doi.org/10.1007/978-981-10-8471-3_49

[2] Alhassani, Athraa & Aljorany, Ala. 2020. Parametric Study on Unconnected Piled Raft Foundation Using Numerical Modelling. *Journal of Engineering*. 26: 156-171. DOI: https://doi.org/10.31026/j.eng.2020.05.11

[3] Alias, A. & Md Noor, Mohd Jamaludin & Jais, I. 2019. Soil Anisotropic Stress-strain Prediction using Normalised Rotational Multiple Yield Surface Framework (NRMYSF) for Compacted Tropical Residual Sandy Soils. *IOP Conference Series: Materials Science and Engineering*. 527: 012018. DOI: https://doi.org/10.1088/1757-899X/527/1/012018.

[4] Al-Taie, Entidhar & Al-Ansari, Nadhir & Knutsson, Sven. 2016. Evaluation of Foundation Settlement under Various Added Loads in Different Locations of Iraq Using Finite Element. *Engineering*. 08: 257-268. DOI: https://doi.org/10.4236/eng.2016.85022.

[5] Asaoka, Akira. 1978. Observational Procedure of Settlement Prediction. Soils and Foundations. 18: 87-101. DOI: https://doi.org/10.3208/sandf1972.18.4_87.

[6] Bungenstab, Felipe & Bicalho, Kátia. 2015. Settlement Predictions of Footings on Sands using Probabilistic Analysis. *Journal of Rock Mechanics and Geotechnical Engineering*. 8. DOI: https://doi.org/10.1016/j.jrmge.2015.08.009.

[7] Das, Braja & Sivakugan, Nagaratnam. 2007). Settlements of Shallow Foundations on Granular Soil - An Overview. *International Journal of Geotechnical Engineering*. 1: 19-29. DOI: https://doi.org/10.3328/IJGE.2007.01.01.19-29.

[8] Foye, K. & Basu, P. & Prezzi, Monica. 2008. Immediate Settlement of Shallow Foundations Bearing on Clay. *International Journal of Geomechanics*. 8: 5(300). DOI: https://doi.org/10.1061/(ASCE)1532-3641(2008)

[9] H. E. Lemmen & Jacobsz, Sw. & Kearsley, Elsabé. 2017. The Influence of Foundation Stiffness on the Behaviour of Surface Strip Foundations on Sand. *Journal of the South African Institution of Civil Engineers*. 59: 19-27. DOI: https://doi.org/10.17159/2309-8775/2017/v59n2a3.

[10] Kim, P., Y. G. Kim, H. B. Myong, C. H. Paek, and J. Ma. 2019. Numerical Analysis for Nonlinear Consolidation of Saturated Soil using Lattice Boltzmann Method. *Int. Res. J. Eng. Technol.* 6(4): 3611-3618.
[11] Kim, Pyol & Ri, Myongchol & Kim, Yong-Gun & Ri, Gunhyang & Myong, Hak-Bom. 2020. One-Dimensional Consolidation Analysis of Unsaturated Soils under Cyclic Loadings. *Shock and Vibration.* 2020: 1-16. DOI: https://doi.org/10.1155/2020/7285323.
[12] Ladd, Charles & Foott, Roger. 1974. New Design Procedure for Stability of Soft Clays. *Journal of Geotechnical Engineering ASCE.* 100: 763-786. DOI: https://doi.org/10.1016/0148-9062(74)90494-X.
[13] Larsson, R., & Mattsson, H. 2003. Settlements and Shear Strength Increase Below Embankments - Long-Term Observations and Measurement of Shear Strength Increase by Seismic Cross-Hole Tomography. Report. Swedish Geotechnical Institute.
[14] Md. Noor, M. J. and Anderson, W. F. 2015. Concept of Effective Stress and Shear Strength Interaction in Rotational Multiple Yield Surface Framework and Volume Change Behaviour of Banting Clay. Recent Advances in Applied and Theoretical Mechanics. *Proceeding of the 11th International Conference on Applied and Theoretical Mechanics (Mechanics' 15)*. *Kuala Lumpur.*
[15] Md Noor, Mohd Jamaludin & Ibrahim, A & Rahman, A. 2018. Normalized Rotational Multiple Yield Surface Framework (NRMYSF) Stress-strain Curve Prediction Method based on Small Strain Triaxial Test Data on Undisturbed Auckland Residual Clay Soils. *IOP Conference Series: Earth and Environmental Science*. 140: 012100. DOI: https://doi.org/10.1088/1755-1315/140/1/012100.
[16] Olson, R. E. 1998. Settlement of Embankments on Soft Clays: (The Thirty-First Terzaghi Lecture). *Journal of Geotechnical and Geoenvironmental Engineering*. 124(8): 659-669. DOI: https://doi.org/10.1061/(asce)1090-0241(1998)124:8(659).
[17] Osman, A. S. & Bolton, M. D. 2004. A New Approach to the Estimation of Undrained Settlement of Shallow Foundations on Soft Clay. Engineering Practice and Performance of Soft Deposits, IS-OSAKA 2004.
[18] Seawsirikul S., Chantawarangul K. and Vardhanabhuti, B. 2015. *Evaluation of Differential Settlement along Bridge Approach Structure on soft Bangkok Clay*. IOP Press. DOI: https://doi.org/10.3233/978-1-61499-580-7-614.
[19] Syahmizzi, A. & Noor, Mohd. 2020. Volume Change Behaviour of Banting Clay by The Concept of Effective Stress and Shear Strength Interaction. *The Journal of the Institution of Engineers, Malaysia*. 80. DOI: https://doi.org/10.54552/v80i2.68.
[20] Terzaghi, K. 1943. *Theoretical Soil Mechanics.* New York: John Wiley.
[21] Ural, N. 2018. The Importance of Clay in Geotechnical Engineering. In (Ed.). Current Topics in the Utilization of Clay in Industrial and Medical Applications. IntechOpen. DOI: https://doi.org/10.5772/intechopen.75817.
[22] Wesley, L., & Pender, M. 2008. Soil Stiffness Measured in Oedometer Test. *Proc. 18th NZGS Geotechnical Symposium on Soil-Structure Interaction.*
[23] Whitlow, R. 2004. *Basic Soil Mechanics*. 4th Edition ed. PEARSON Prentice Hall.
[24] Young, S & Ismail, G & Chong, Abraham. 2019. Towards Innovative Design and Construction Standards for Lime Stabilized Subgrades. *IOP Conference Series: Materials Science and Engineering*. 512: 012028. DOI: https://doi.org/10.1088/1757-899X/512/1/012028.
[25] Z. hang, Wei Min. 2017. A Simple Method for Rate of Consolidation Deformation and Its Applications. *Proceedings of the 19th International Conference on Soil Mechanics and Geotechnical Engineering, Seoul.*